Title: Quarterly Report for LANL Activities: FY12-Q2 National Risk Assessment Partnership (NRAP): Industrial Carbon Capture Program

Author(s): Pawar, Rajesh J.

Intended for: Quarterly progress report for funding agency
Report

LA-UR-Draft

Quarterly Report for LANL Activities: FY12-Q2

National Risk Assessment Partnership (NRAP): Industrial Carbon Capture Program

Report Date: April 11, 2012
Report Period: Jan – Mar 2012

WORK PERFORMED UNDER AGREEMENT

FWP FE-102-002-FY10

SUBMITTED BY

Los Alamos National Laboratory
P.O. 1663
Los Alamos, NM 87545

PRINCIPAL INVESTIGATOR

Rajesh Pawar

Contributors:

Bill Carey, Elizabeth Keating, Phoolendra Mishra, Dennis Newell, George Zyvoloski

PROGRAM MANAGER

Melissa Fox

SUBMITTED TO

U. S. Department of Energy
National Energy Technology Laboratory

Executive Summary:

This report summarizes progress of LANL activities related to the tasks performed under the LANL FWP FE102-002-FY10, National Risk Assessment Partnership (NRAP): Industrial Carbon Capture Program. This FWP is funded through the American Recovery and Reinvestment Act (ARRA). Overall, the NRAP activities are focused on understanding and evaluating risks associated with large-scale injection and long-term storage of CO_2 in deep geological formations. One of the primary risks during large-scale injection is due to changes in geomechanical stresses to the storage reservoir, to the caprock/seals and to the wellbores. These changes may have the potential to cause CO_2 and brine leakage and geochemical impacts to the groundwater systems. While the importance of these stresses is well recognized, there have been relatively few quantitative studies (laboratory, field or theoretical) of geomechanical processes in sequestration systems. In addition, there are no integrated studies that allow evaluation of risks to groundwater quality in the context of CO_2 injection-induced stresses. The work performed under this project is focused on better understanding these effects. LANL approach will develop laboratory and computational tools to understand the impact of CO_2-induced mechanical stress by creating a geomechanical test bed using inputs from laboratory experiments, field data, and conceptual approaches. The Geomechanical Test Bed will be used for conducting sensitivity and scenario analyses of the impacts of CO_2 injection. The specific types of questions will relate to fault stimulation and fracture inducing stress on caprock, changes in wellbore leakage due to evolution of stress in the reservoir and caprock, and the potential for induced seismicity. In addition, the Geomechanical Test Bed will be used to investigate the coupling of stress-induced leakage pathways with impacts on groundwater quality.

LANL activities are performed under two tasks: 1) develop laboratory and computational tools to understand CO_2-induced mechanical impacts and 2) use natural analog sites to determine potential groundwater impacts. We are using the Springerville-St. John Dome as a field site for collecting field data on CO_2 migration through faults and groundwater impacts as well as developing and validating computational models.

During the FY12 second quarter we have been working with New England Research Company to construct a tri-axial core-holder. We have built fluid control system for the coreflood system that can be ported to perform in-situ imaging of core. We have performed numerical simulations for groundwater impacts of CO_2 and brine leakage using the reservoir model for Springerville-St John's Dome site. We have analyzed groundwater samples collected from Springerville site for major ion chemistry and isotopic composition. We are currently analyzing subsurface core and chip samples acquired for mineralogical composition.

Progress:

Task 1 Develop laboratory and computational tools to understand CO_2-induced mechanical impacts (Task Leads: Bill Carey, George Zyvoloski):

We are in the process of building our triaxial system in coordination with the vendor constructing the triaxial coreholder. The vendor (New England Research) has supplied us with detailed AutoCAD drawings for the triaxial coreholder. We have approved these and the coreholder is under construction. A schematic of the coreholder is shown in Figure 1. This shows the key elements of the device including the floating piston for delivering the axial load, transducers for recording acoustic velocities, ports for injection of CO_2-brine mixtures, and an aluminum body to allow for tomographic imaging.

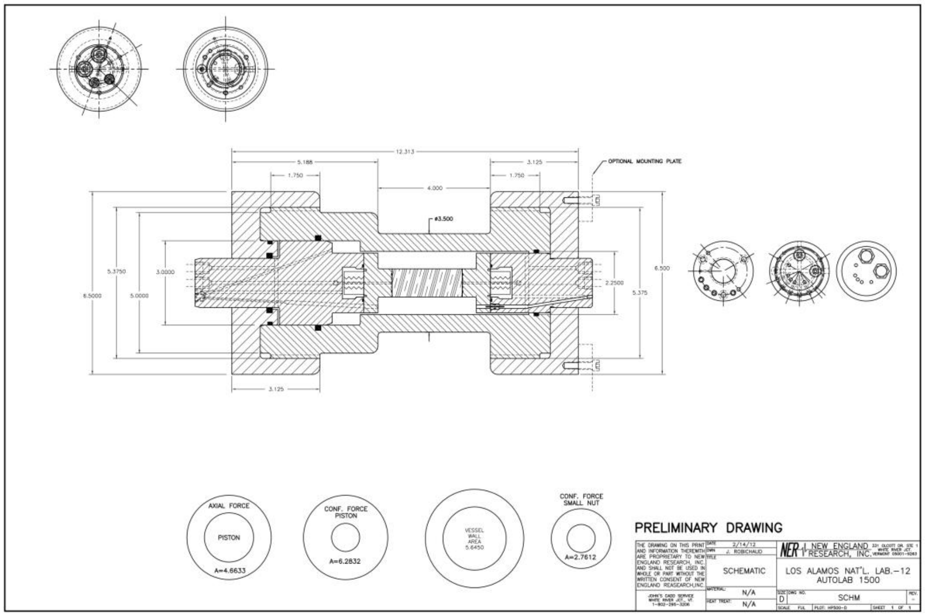

Figure 1. Detailed drawing of the triaxial coreholder for use in the triaxial tomographic coreflood system. The unit is under construction at New England Research.

We have designed the auxiliary fluid control system. We will use a set of three mobile carts to hold all of the equipment that is part of the triaxial coreflood system. The carts are on wheels and each will be of a manageable size to allow transport to and from the beam line as needed. Two carts will hold the pumping system for CO_2 and brine, respectively (includes the pumps, accumulators, and tubing). The third cart will have the coreholder, the backpressure regulator, and the axial and confining pressure pumps. A photograph of a partly assembled cart is shown in Figure 2. This shows the brine pumping system, which consists of two interconnected pumps for maintaining steady delivery of brine. In the third quarter, we will complete assembly of the carts and auxiliary equipment and take delivery of the triaxial coreholder.

Task 2 Use natural analog sites to determine potential geochemical impacts (Leads: Dennis Newell, Elizabeth Keating):

A suite of simulations has been performed to investigate plausible mechanisms and CO_2 and/or brine at the Springerville-St.Johns natural analog site.

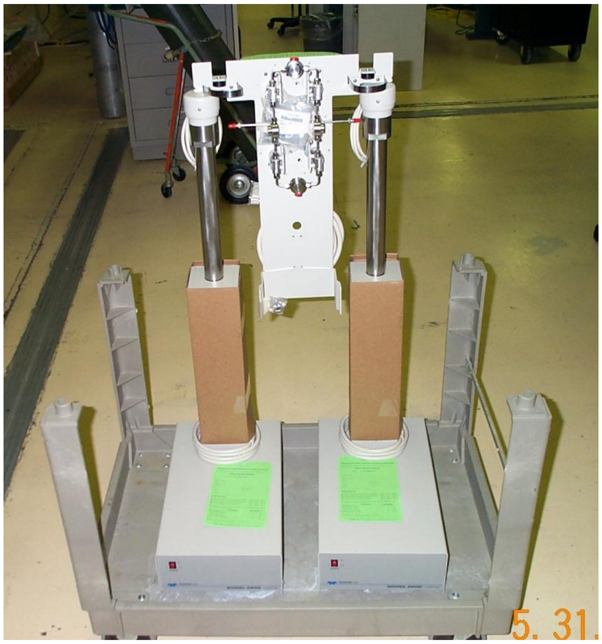

Figure 2. Mobile cart with two pumps and switching relay for delivering brine to the triaxial coreholder system. The cart is partially constructed. (The date on the photograph is incorrect.)

a. 3-D flow simulations. The purpose of these simulations is to determine if the measured water level data can provide quantitative information about the permeability structure of the subsurface, including the Coyote Wash fault zone. A flow model using heterogeneity based on the Geologic Framework Model (GFM) for the site. The narrow fault represented in the GFM was widened to account for the conceptual model that the entire production wellfield used by Tuscon Electric Power (TEP) is within a relatively high permeability fault zone. The groundwater extractions reported by TEP were tabulated and specified as transient boundary conditions (Figure 3).

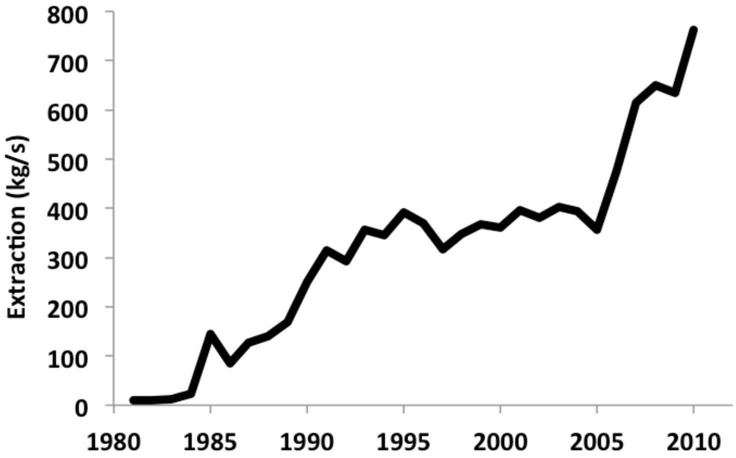

Figure 3. History of groundwater extraction by Tuscon Electric Power Company at Springerville-St. Johns.

The regional and local water level data was used to define model boundaries (Figure 4) and to define calibration targets. An automated parameter estimation software package (PEST) is being used to find permeability and specific storage values that are consistent with the water level data. Although the calibration is not complete, it is very clear from preliminary results that the fault zone containing the TEP well-field must be relatively high permeability (~ $10^{11} – 10^{12}$ m^2). The work is ongoing.

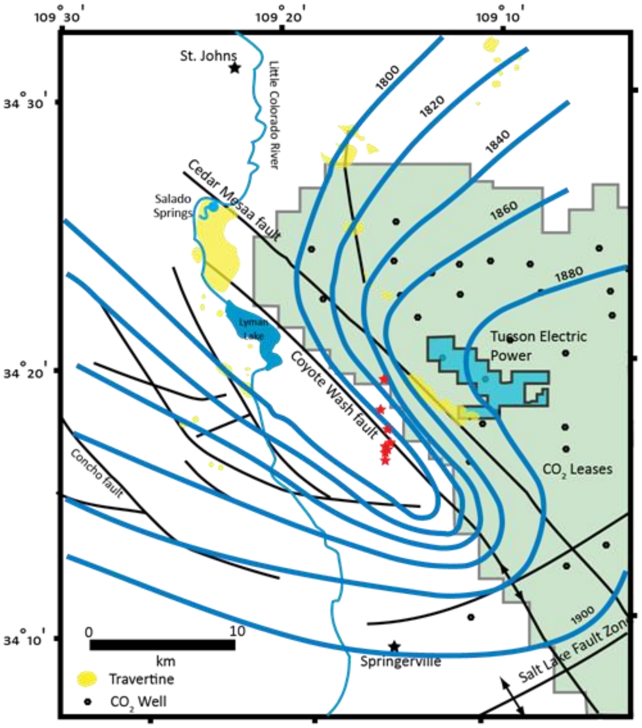

Figure 4. Site map of study area at Springerville-St Johns. Water levels are indicated by blue contours. Red dots show wells sampled. Red box illustrates extent of numerical model.

b. Idealized 1-D CO_2/brine transport within a fault zone. The purpose of these simulations is to investigate possible flow and transport mechanisms controlling CO_2 and/or brine in the Coyote Wash fault system. The simulations utilize LANL's multi-phase heat and mass flow simulator FEHM to simulate multi-component (CO_2, water, NaCl) flow and transport. The density of water is dynamically calculated according to spatially and temporally varying pressure, temperature, salt concentration (Haas 1976), and dissolved CO_2 concentration (Garcia, 2001). The solubility of CO_2 is controlled by pressure, temperature, and salt concentration using the formulation of Duan and Sun (2003).

First, idealized multiphase discharge along a fault zone is simulated, based on the geometry proposed by Pruess (2002). The zone is 500m thick and 25m wide. Initial hydrostatic conditions are calculated using an upper boundary condition of P = 1MPa, and uniform temperature of 40 ^{o}C. Under these conditions free CO_2 will be in the supercritical phase at $z < 270$m and in the gas phase at higher elevations. A linear relative permeability and capillary pressure relationship with minimum residual water saturation of 0.1 is assumed. The fault is fully water saturated at time=0 with a brine (1M NaCl) below 100m and freshwater elsewhere. At the beginning of the transient simulations, a flux of 0.012 kg/s CO_2 is applied at the base of the fault. In Figure 5, vertical profiles of sodium concentration, total CO_2 mass, and dissolved mass fractions are shown at various times. It is evident that CO_2 can migrate up the fault zone without entraining the brine. The vertical extent of the brine front remains virtually unchanged throughout the simulation. The highest dissolved mass fraction of CO_2 exists at intermediate depths, where solubility is enhanced by low salt concentrations and relatively high pressures.

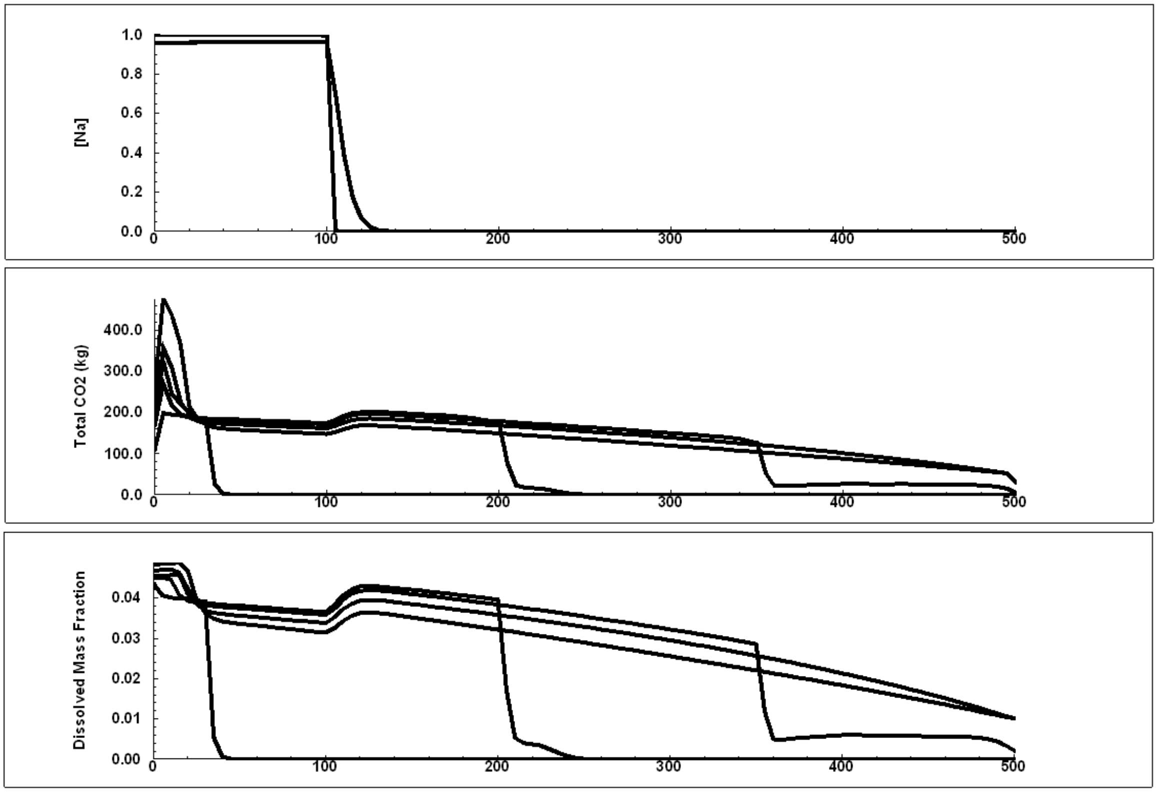

Figure 5. Profiles of a) dissolved sodium (moles/kg), b) total CO_2 (kg), and c) dissolved CO_2 mass fraction at several times (10, 90, 150, 200, and 290 days).

c. 3-D CO_2/brine transport at the field scale. These simulations are intended to develop hypotheses concerning migration of CO_2 in the shallow aquifer at Springerville and the absence of increasing salinity, despite extensive groundwater extraction. Three-dimensional simulations were conducted at a scale roughly corresponding to the Springerville-St John site (Figure 4). The initial simulations are based on a simplified structure, rather than the GFM-based model. A simple permeability structure is imposed, as shown in cross-section in Figure 6. A shallow aquifer (1500 m – 1850 m) is separated by the storage reservoir (1000 m – 1500m) by an aquitard. The aquitard is breached by a relatively permeable vertical fault zone. In order to develop reasonable values of permeability for the aquifer units, the reported groundwater extractions (Figure 4) were applied and permeabilities were adjusted until the model was in agreement with the measured drawdowns. Table 1 lists resulting model parameters for the calibrated model and the suite of simulations described below.

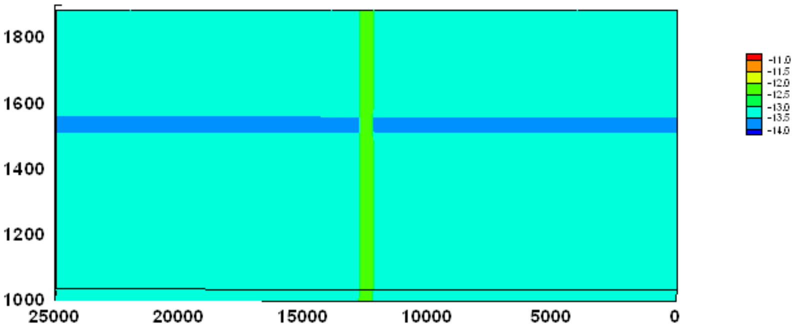

Figure 4. Cross-section through numerical model. Colors indicate permeability (log m^2).

A hydrostatic water-only equilibrium was calculated for the system, assuming the lower reservoir ($z <= 1300m$) is occupied by a 0.5M NaCl water and 'pure' water elsewhere. The upper surface was initialized to a pressure of 1.MPa; a row of nodes at the north end of the fault zone (roughly corresponding to Salido Springs area, a regional discharge) was specified as constant pressure (1 MPa). The upper surface was initialized to 20 °C with a geothermal gradient of 35 °C/km at depth. A transient simulation followed, with specified CO_2 flux uniformly distributed along the base of the model (total flux = (441 X 0.1 = 44.1 kg/s). The results are, in many ways, similar to the 1-D fault simulations described above. Dissolved CO_2 is transported readily through the fault zone (Figure 7a). Liquid CO_2 saturations (not shown) are always quite low (< .5E-3). Significant gas saturations do develop, however, at shallow depths (Figure 7b). Spatial extent of brackish waters (not shown) does not change significantly during the simulations.

Field Studies

Groundwater samples collected from Tucson Electric Power (TEP) wells and Salado springs at Springerville-St. Johns Dome during November of 2011 (Figure 8) have been analyzed for major and trace element chemistry and for carbon, oxygen and hydrogen isotopes. TEP groundwater production wells (P-series, Table 1 and 2) are completed into the regional aquifer (Glorieta Sandstone; also known as Coconino aquifer) and utilized for power production. These wells are located to the west of the Cedar Mesa anticline/fault (Figure 8). Wells that TEP installed to the east of the anticline do not produce adequate water for power production. We interpret that wells located west of the anticline are completed into a fracture zone associated with the Coyote Wash fault, and that the higher production of groundwater is related to increased permeability in the fractured fault zone.

Groundwater samples actively degassed (effervesced) during sampling, and it is assumed that was due to elevated pCO_2 in the groundwater. The impact of elevated pCO_2 is apparent due to slightly acidic field pH of the water and elevated bicarbonate (HCO_3) content over typical dilute surface and groundwater (Table 1). Most samples also show elevated concentrations of all major elements

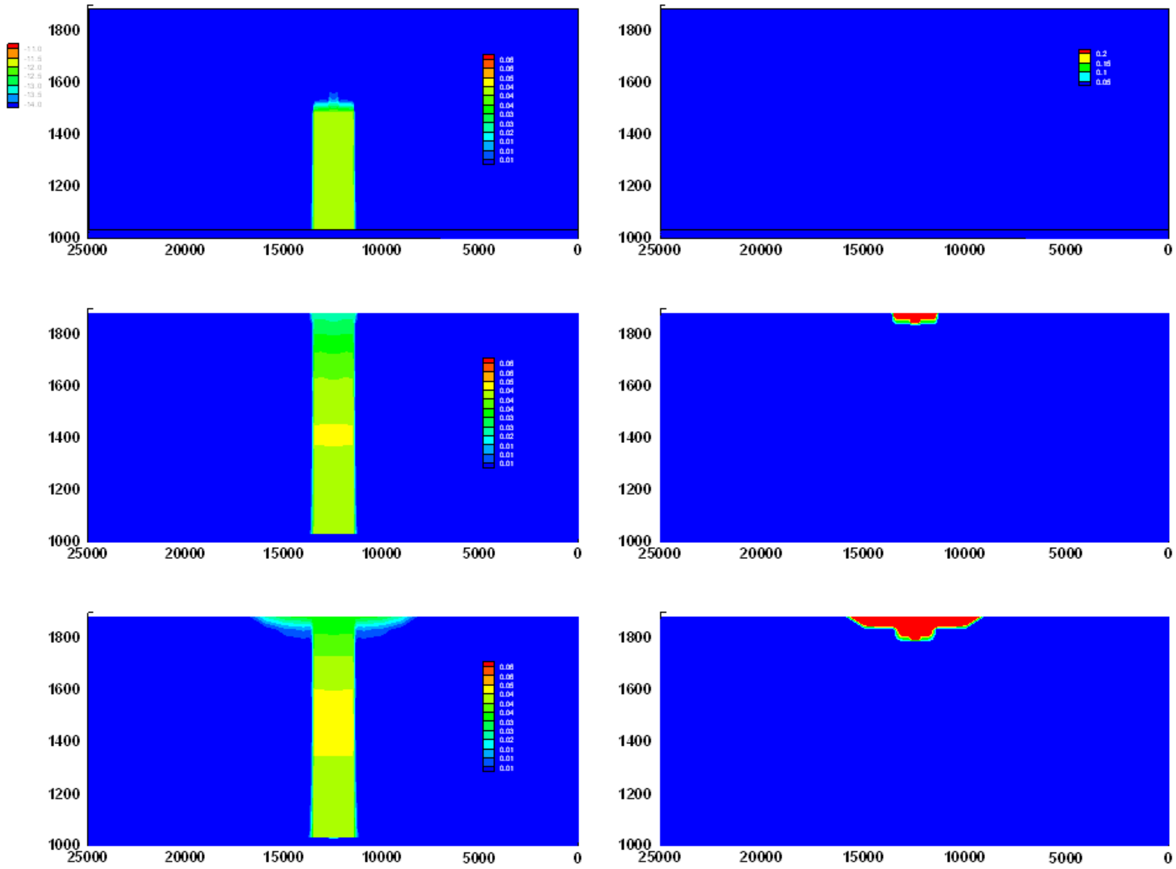

(a) (b)

Figure 7. a) Dissolved CO_2 mass fraction at different times. Note the maximum concentrations are at intermediate depths, due to salinity and pressure affects. b) Gas phase CO_2 saturations at different times.

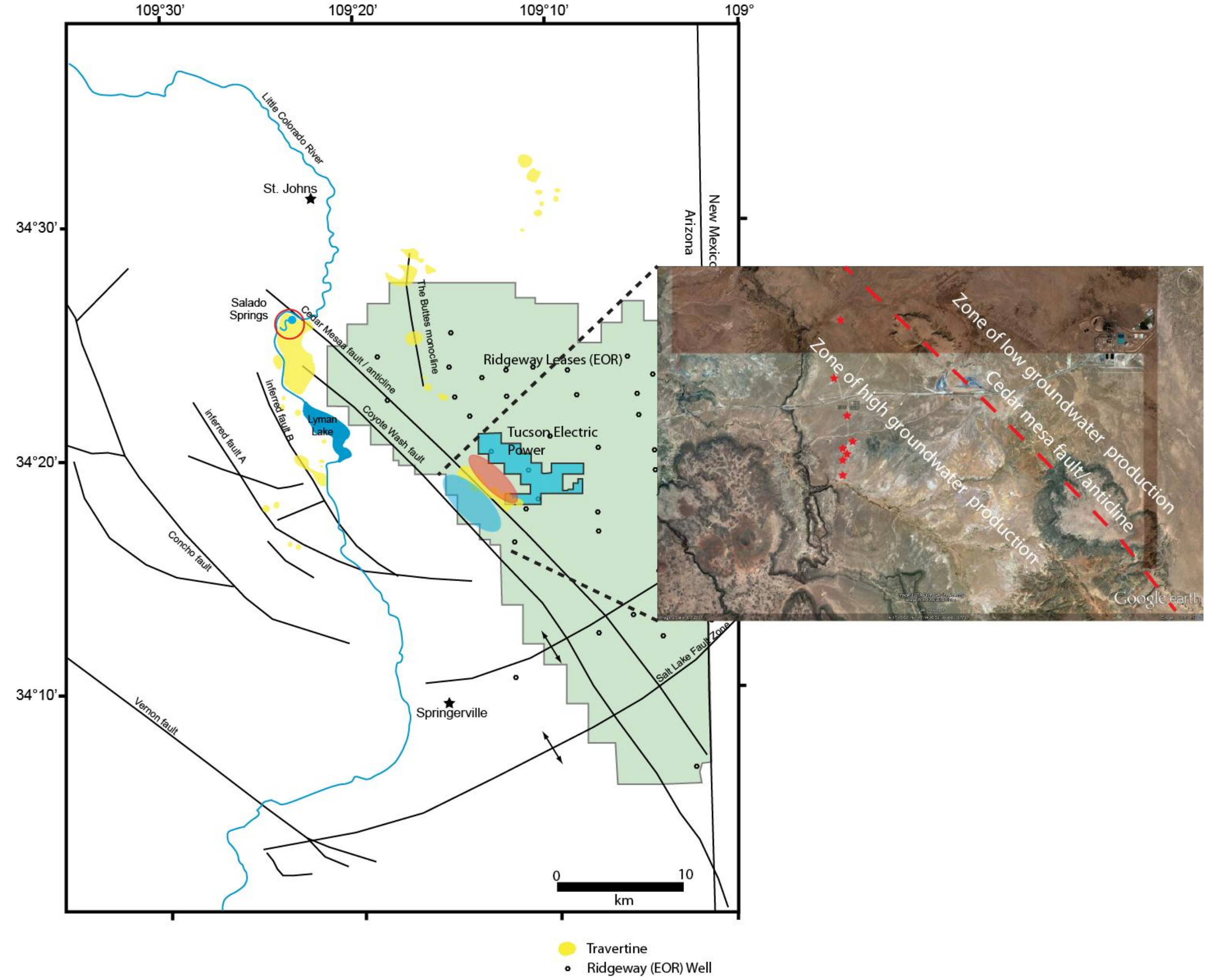

Figure 8. Location of wells (stars) and Salado springs that were sampled in November 2011. Note the zones of high and low groundwater production located west and east of the Cedar Mesa Anticline, respectively.

Table 1. Major element chemistry from TEP P-wells and Salado Springs.

Sample ID	Ca	Cl	HCO_3	K	Mg	Na	SO_4	pH field	pH lab
P-19	188	215	559	20	50	211	402	6.59	7.44
Salado Spring 2	309	449	758	26	59	380	707	6.19	7.32
State Well at Salado spring	307	449	769	27	60	387	688	6.20	7.28
P-10a	184	213	563	17	45	205	379	6.30	7.22
P-18	301	414	710	26	58	338	692	6.65	7.35

P-20	163	175	516	16	42	166	323	6.37	7.38
P-16	139	138	467	12	41	137	252	6.87	7.27
P-7a	135	146	458	10	39	131	259	6.88	7.59
Salado Spring 1	322	473	744	25	61	359	710	6.10	7.27
P-9a	315	491	754	27	54	382	710	6.42	7.62
P-9	307	499	631	32	55	413	723	nd	7.44
P-8a	165	190	522	17	45	182	345	6.32	7.54

concentrations in mg/l

nd – not determined

Table 2. Minor and trace element chemistry from TEP P-wells and Salado Springs

Sample ID	As	B	Ba	Br	Cs	Cu	F	Fe	Li	Mn	Ni
P-19	0.016	0.79	0.022	0.2	0.02	<0.01	1.8	0.4	0.25	0.02	<0.01
Salado Spring 2	0.009	0.88	0.015	0.2	0.03	<0.01	2.2	<0.1	0.50	0.02	<0.01
State Well at Salado spring	0.021	0.81	0.015	0.3	0.03	<0.01	2.1	15	0.53	0.15	0.01
P-10a	0.018	0.46	0.023	<0.1	0.02	<0.01	1.9	0.2	0.26	0.02	<0.01
P-18	0.035	0.71	0.016	0.1	0.03	<0.01	2.6	0.8	0.47	0.03	<0.01
P-20	0.014	0.41	0.024	<0.1	0.02	<0.01	2.2	0.2	0.23	0.02	<0.01
P-16	0.011	0.35	0.025	<0.1	0.02	<0.01	1.9	0.3	0.18	0.01	<0.01
P-7a	0.003	0.30	0.023	<0.1	0.02	<0.01	1.8	<0.1	0.18	0.01	0.08
Salado Spring 1	0.016	0.75	0.017	0.2	0.03	<0.01	2.3	<0.1	0.55	0.03	<0.01
P-9a	0.042	0.77	0.019	<0.1	0.04	<0.01	1.9	0.8	0.57	0.04	<0.01
P-9	0.007	1.13	0.019	0.1	0.04	0.02	2.1	<0.1	0.60	0.04	0.02
P-8a	0.012	0.53	0.022	<0.1	0.02	<0.01	2.3	0.3	0.24	0.01	<0.01

concentrations in mg/l

compared to what would be expected from a sandstone-hosted shallow aquifer. With the exception of arsenic, minor and trace elements do not appear anomalous (Table 2). Arsenic exceeds the EPA drinking water limit (10 ppb; ~0.010 mg/l) in 9 of the 12 samples, with a maximum of 0.042 mg/l (42 ppb) at P-9a. Chemically, the groundwater at Salado springs is very similar to the groundwater hosted in the Glorieta sandstone, supporting the hypothesis that the springs are a local discharge point for the aquifer.

Stable isotopes of oxygen, hydrogen and carbon are presented in Figures 9 and 10. Results are reported in delta notation (e.g., $\delta^{18}O$), with the units of per mil versus the international standards VSMOW for hydrogen and oxygen, and VPDB for carbon.

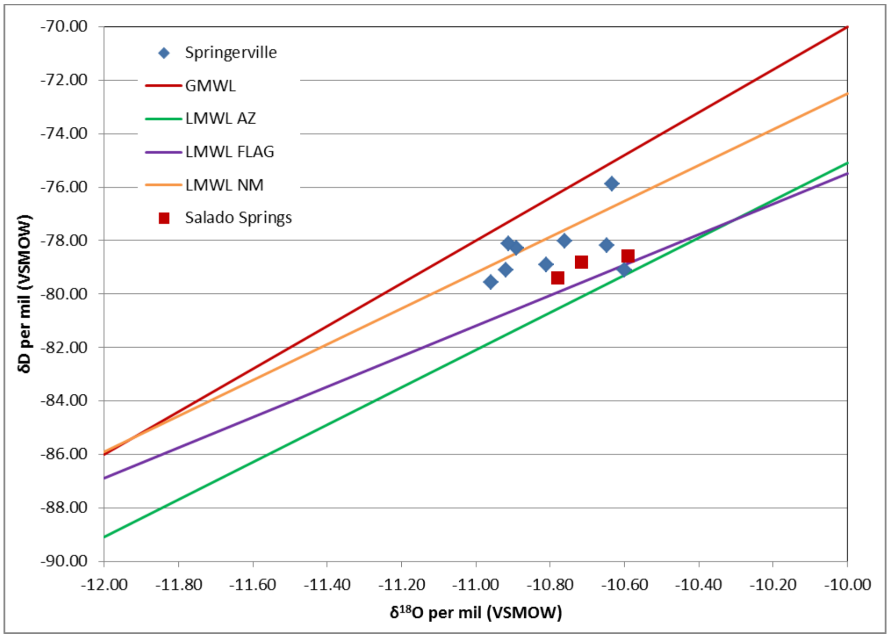

Figure 9. δD vs. $\delta^{18}O$ for the TEP wells (Springerville) and Salado Springs. The global meteoric water line (GMWL) and local meteoric water lines (LMWL) for New Mexico, Arizona and Flagstaff, AZ are shown for reference (after Kendall and Coplen, 2001).

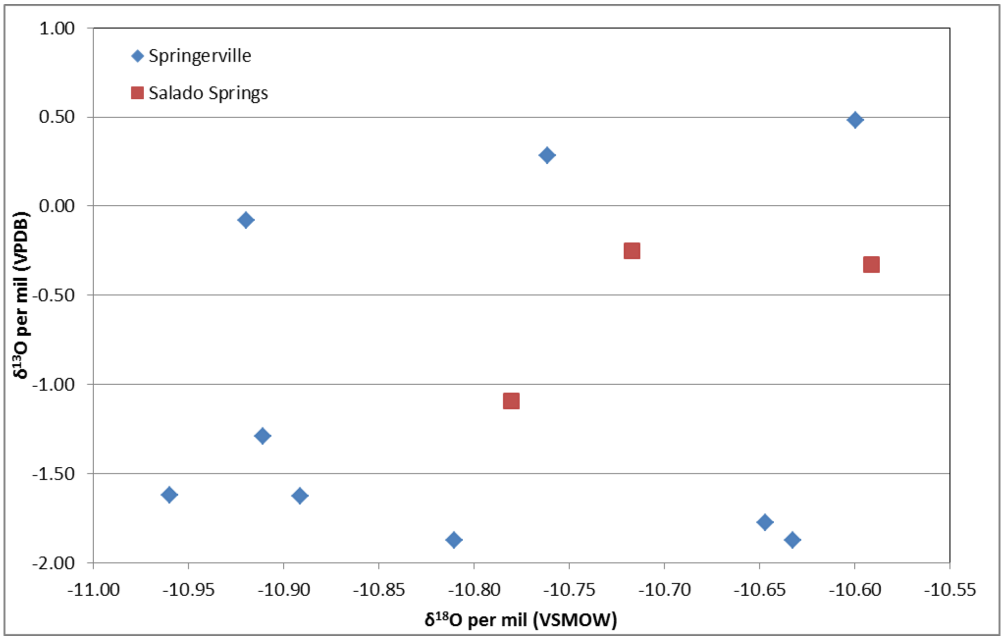

Figure 10. $\delta^{13}C$ of dissolved inorganic carbon vs. $\delta^{18}O$ for the TEP wells (Springerville) and Salado Springs.

Subsurface core and chip samples acquired from the Arizona Geological Survey are currently being analyzed for mineralogical composition by X-ray Diffraction, and we are starting trace element analysis of these samples. Thin sections prepared from these core and chip samples have been received and are undergoing optical microscopic analysis. Subsequent SEM analysis of these sections is planned.

Stable isotope compositions of hydrogen and oxygen indicate that the groundwater is meteoric in origin, similar to the local meteoric water found in the region. It does not appear that CO_2 addition from the dome has impacted these isotopes. However, carbon isotope compositions are much higher compared to typical groundwater. Typical groundwater with dissolved inorganic carbon compositions controlled by equilibration with soil gas would generally have $\delta^{13}C$ values less than -10 per mil. Springerville groundwater values range from -2 to +0.5 per mil indicating that introduction of CO_2 from the dome with high $\delta^{13}C$ has significantly modified that dissolved inorganic carbon composition.

References

Kendall, C., and Coplen, T.B., 2001, Distribution of oxygen-18 and deuterium in river water across the United States: Hydrologic Processes, v. 15, p. 1363-1393.

Milestones and Status:

1.1: Acquire triaxial core flood system (Completion Date: 5/31/2012)

Status: Delayed due to setback in vendor contract negotiations

1.2: Complete geomechanical flow-through experiments: caprock (Completion Date: 9/30/2012)

Status: not started.

1.3: Complete geomechanical flow-through experiments: wellbore materials (Completion Date: 9/30/2013)

Status: not started.

2.1: Complete geomechanical simulations (Completion Date: 9/30/2013)

Status: Initiated.

2.2: Create geomechanical test bed (Completion Date: 6/30/2012)

Status: Initiated

2.3: Sensitivity and scenario analysis (Completion Date: 9/30/2013)

Status: not started.

3.1: Baseline predictive reactive-transport model for natural analog site (Completion Date: 9/30/2012)

Status: Initiated.

3.2: Groundwater chemistry observations at a natural analog site, compared to reactive-transport (Completion Date: 9/30/2012)

Status: initiated.

3.3: Assessment of predictive capability of reactive-transport models and value of information assessment (Completion Date: 9/30/2013)

Status: not started.